J Neurophysiol 118: 3118–3131, 2017.
First published August 30, 2017; doi:10.1152/jn.00521.2017.

RESEARCH ARTICLE | *Sensory Processing*

Contribution of spiking activity in the primary auditory cortex to detection in noise

Kate L. Christison-Lagay,[1]* Sharath Bennur,[1]* and Yale E. Cohen[1,2,3]
[1]*Department of Otorhinolaryngology, University of Pennsylvania, Philadelphia, Pennsylvania;* [2]*Department of Neuroscience, University of Pennsylvania, Philadelphia, Pennsylvania; and* [3]*Department of Bioengineering, University of Pennsylvania, Philadelphia, Pennsylvania*

Submitted 10 July 2017; accepted in final form 27 August 2017

Christison-Lagay KL, Bennur S, Cohen YE. Contribution of spiking activity in the primary auditory cortex to detection in noise. *J Neurophysiol* 118: 3118–3131, 2017. First published August 30, 2017; doi:10.1152/jn.00521.2017.—A fundamental problem in hearing is detecting a "target" stimulus (e.g., a friend's voice) that is presented with a noisy background (e.g., the din of a crowded restaurant). Despite its importance to hearing, a relationship between spiking activity and behavioral performance during such a "detection-in-noise" task has yet to be fully elucidated. In this study, we recorded spiking activity in primary auditory cortex (A1) while rhesus monkeys detected a target stimulus that was presented with a noise background. Although some neurons were modulated, the response of the typical A1 neuron was not modulated by the stimulus- and task-related parameters of our task. In contrast, we found more robust representations of these parameters in population-level activity: small populations of neurons matched the monkeys' behavioral sensitivity. Overall, these findings are consistent with the hypothesis that the sensory evidence, which is needed to solve such detection-in-noise tasks, is represented in population-level A1 activity and may be available to be read out by downstream neurons that are involved in mediating this task.

NEW & NOTEWORTHY This study examines the contribution of A1 to detecting a sound that is presented with a noisy background. We found that population-level A1 activity, but not single neurons, could provide the evidence needed to make this perceptual decision.

auditory cortex; rhesus monkey; hearing in noise; behavior

HEARING IN NOISE is one of the fundamental challenges for the auditory system and is one that normal-hearing listeners can easily perform (Bronkhorst 2000; Bronkhorst and Plomp 1992; Moore et al. 2014; Narayan et al. 2007; Shetake et al. 2011). For example, listeners can readily hear a friend's voice at a party, even in a noisy background filled with the voices of other speakers, music, and clinking glasses. In visual neuroscience, an analogous problem is referred to as "foreground-background segregation" (Pomeranz and Kubovy 1986).

Neural correlates of hearing in noise have been identified throughout the central auditory system (Bar-Yosef and Nelken 2007; Delgutte and Kiang 1984; Giraud et al. 1997; May et al. 1998; Mesgarani et al. 2014; Narayan et al. 2007; Schneider and Woolley 2013; Scott and McGettigan 2013; Shetake et al. 2011; Wong et al. 2008). Yet, to our knowledge, the direct relationship between the spiking activity of individual cortical neurons and the behavioral reports of listeners detecting sounds in background noise is unknown. In this study, we partially filled this knowledge gap by recording A1 spiking activity while monkeys detected a target stimulus that was presented with a noisy background.

We targeted A1 because it is situated at the beginning of the ventral auditory pathway. Auditory perception is thought to be mediated by the neural computations in this pathway, which includes A1, belt and parabelt regions of the auditory cortex, and the ventrolateral prefrontal cortex (Bizley and Cohen 2013; Rauschecker and Scott 2009; Romanski 2007; Tsunada et al. 2016). Work from our group has shown that spiking activity in the auditory cortex provides sensory evidence for a perceptual decision but does not seem to correlate directly with behavioral choice (Tsunada et al. 2011, 2012, 2016), whereas prefrontal spiking activity is modulated by behavioral choice (Lee et al. 2009; Russ et al. 2008b). In contrast to this work from our laboratory, important work from other groups has identified choice-related modulations in both spiking activity and in field potentials in the primary auditory cortex (Bizley et al. 2013; Niwa et al. 2012b, 2013), consistent with a broader literature indicating that A1 has an important role in perception and behavior (King and Nelken 2009; Sutter and Shamma 2011).

To further understand A1's contribution to perception and behavior, we recorded spiking activity from A1 while monkeys reported (i.e., detected) the presence of a "target" stimulus (i.e., a tone burst) that was presented with a background of comodulated broadband noise. It is worth noting that this study differs from a related study by Sutter and colleagues (Johnson et al. 2012; Niwa et al. 2012a, 2012b), who tested the neural correlates of a monkey's ability to detect whether or not a noise burst was amplitude modulated. In contrast, the focus in our current study was on the ability of a listener to detect an unmodulated tone in a modulated noise background. We found that the spiking activity of the median A1 neuron was not modulated by the stimulus- and task-related parameters of our task. Instead, we found more robust representations of these parameters when we considered population-level A1 spiking activity: small populations of A1 neurons mirrored the behavioral sensitivity of the monkeys. Together, these findings are

* K. L. Christison-Lagay and S. Bennur contributed equally to this work.

Address for reprint requests and other correspondence: Y. E. Cohen, Dept. of Otorhinolaryngology, 3400 Spruce St.-5 Ravdin, Philadelphia, PA 19104 (e-mail: ycohen@pennmedicine.upenn.edu).

consistent with the hypothesis that the sensory evidence, which is needed to detect a target stimulus in a noisy background, is represented in population-level A1 activity and may be assessable by downstream neurons that are involved in mediating this task.

MATERIALS AND METHODS

The University of Pennsylvania Institutional Animal Care and Use Committee approved all experimental protocols. All surgical procedures were conducted under general anesthesia, using aseptic surgical techniques.

Experimental Chamber

Behavioral training and neural recording sessions were conducted in a radiofrequency (RF)-shielded, darkened room with sound-absorbing walls. During each session, a male monkey [*Macaca mulatta*; *monkey S* (age 12 yr) or *monkey A* (age 8 yr)] was seated in a primate chair in the center of the room. A calibrated speaker (model MSP7; Yamaha) was placed in front of the monkey at a distance of 1.5 m and at eye level. A touch-sensitive lever was attached to the primate chair; the monkey released the lever with his right hand to indicate his behavioral report. Auditory stimuli were synthesized using MATLAB (The MathWorks) and the RX6 digital-signal-processing platform (TDT). Auditory stimuli were transduced by the Yamaha speaker.

Identification of A1

From MRI images of each monkey's brain, A1's anatomical location on the surface of the superior temporal gyrus (*monkey S*, left hemisphere; *monkey A*, left hemisphere) was identified using the Brainsight (Rogue Technologies) software package (Fig. 1). A1 was further defined by its auditory-response properties (e.g., response latency and frequency-tuning bandwidth) (Camalier et al. 2012; Fu et al. 2004; Kajikawa et al. 2005; Kikuchi et al. 2010; Massoudi et al. 2015; O'Connell et al. 2014; Recanzone et al. 2000; Werner-Reiss and Groh 2008).

Auditory Paradigms and Stimuli

In the passive-listening paradigm, we recorded A1 spiking activity while monkeys listened passively to different frequency tone bursts (Tsunada et al. 2016). From the recorded spiking activity, we calculated the best frequency of an A1 recording site. As described below, the best frequency of each recording site was integrated into the target-in-noise task. The target-in-noise task tested the ability of a monkey to detect a "target" stimulus that was presented with a noisy background. Further details regarding these tasks and stimuli can be found below.

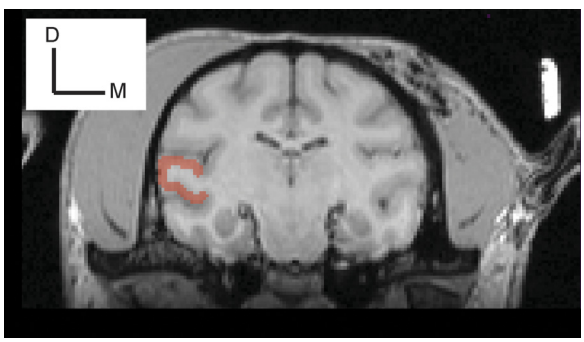

Fig. 1. Recording location. An MRI coronal image of *monkey S*. The area highlighted in red is the superior temporal gyrus. Using the Brainsight (Rogue Technologies) software package, we targeted the middle and dorsal aspect of this gyrus. D, dorsal; M, medial.

Passive-listening paradigm. A monkey listened passively to tone bursts (100-ms duration with a 5-ms $\cos^2$ ramp; 50–80 dB SPL; 400-ms inter-tone-burst interval) with different frequencies (0.5–8.0 kHz in 1/32-octave steps). The sound level and the frequency of the tone bursts were presented in a random order. The monkeys did not receive any juice rewards or any other behavioral feedback during the passive-listening paradigm. From the collected neural data, we calculate the site's best frequency. The best frequency was the frequency value, at the lowest sound level, that elicited a reliable response.

Target-in-noise task. In the target-in-noise task (Fig. 2*A*), there were two types of trials: "target in noise" and "noise only." The behavioral requirements of the noise-only trials were different from those of the target-in-noise trials. Both trials started with a monkey grasping the touch-sensitive lever. In target-in-noise trials, we next presented the target stimulus concurrently with the noise stimulus. The monkey was required to maintain his grip on the lever during presentation of this target-in-noise stimulus and release it within 750 ms of stimulus offset. In noise-only trials, we first presented only the noise stimulus. The monkey was required to maintain his grip on the lever during presentation of this noise-only stimulus and for an additional 750 ms. Next, we presented a "respond" stimulus (a 65-dB SPL tone burst at the site's best frequency), which signaled the monkey to release the lever. We presented the respond stimulus to ensure that the monkey had to perform an action (i.e., release the lever) on every trial to get a reward and could not simply hold the lever to get a reward (see *Trial outcomes and reward structure*). Also, for both trial types, the monkeys were only allowed to release the lever after stimulus onset. Consequently, this was not a reaction-time task.

The target stimulus was a tone burst (750-ms duration; 5-ms $\cos^2$ ramp) that was presented at the best frequency of each recording site (or average best frequency if multiple neurons were isolated from a single recording penetration). The noise-only stimulus was comodulated broadband noise (0.1–16 kHz); this frequency range exceeds the range of monkeys' best hearing (Pfingst et al. 1975). Comodulated noise was generated by multiplying unmodulated noise with a 20-Hz sinusoidal envelope (Fig. 2*B*) (Las et al. 2005; Nelken et al. 1999); this stimulus is equivalent to 100% sinusoidally amplitude modulated noise. The phase relationship between the target and noise-only stimulus was constant. The modulation phase was the same on every trial, but we used fresh noise tokens on every trial. The overall power of the noise-only stimulus was 65 dB SPL (Narayan et al. 2007).

During target-in-noise trials (Fig. 2*A*), we varied the sound level of the target stimulus in 5-dB steps between 60 and 85 dB SPL. As a result, the "target-in-noise ratio" (TNR) was between −5 and +20 dB. This range of sound levels and TNR values was kept constant across all recording sessions. During noise-only trials (Fig. 2*A*), the noise-only stimulus, as noted above, was presented at 65 dB SPL.

Trial outcomes and reward structure. During target-in-noise trials, if the monkey released the lever within 750 ms of offset of the stimulus (median release time: 390 ms), the monkey received a juice reward; this constituted a "hit." If the monkey did not release the lever within 750 ms, this constituted a "miss." During noise-only trials, if the monkey maintained his grip on the lever through the noise and released the lever within 750 ms of offset of the respond stimulus, he received a reward; this constituted a "correct rejection." If he released the lever following offset of the noise-only stimulus, this was a "false alarm." We did not analyze those trials when a monkey released the lever during presentation of the target-in-noise or noise-only stimuli or when he did not release the lever following offset of the respond stimulus.

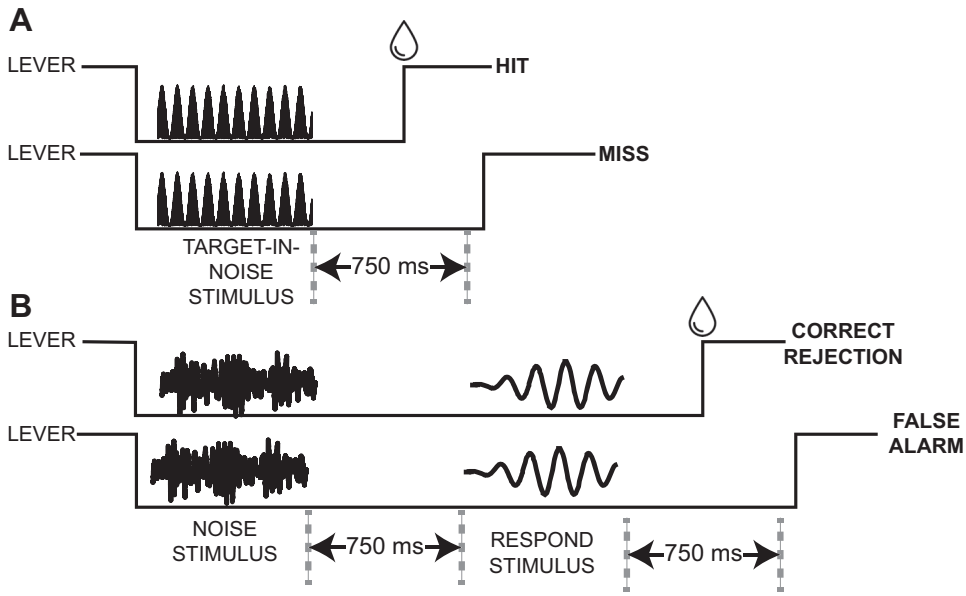

Fig. 2. Schematics of the target-in-noise task. During target-in-noise trials (*A*), a 750-ms auditory stimulus was presented; the "target-in-noise" stimulus was a tone burst that was presented with comodulated noise (100% sinusoidal amplitude modulated noise). If a monkey released a touch-sensitive lever within 750 ms of offset of this stimulus, we classified the trial as a "hit" and the monkey received a reward (water drop; *top*). If he did not release the lever or released it after 750 ms (as depicted), it was classified as a "miss" (*bottom*). During noise-only trials (*B*), a 750-ms comodulated noise burst was first presented. The monkeys had to maintain their grip on the lever during presentation of the noise and for an additional 750 ms. Next, a "respond" stimulus (i.e., a tone burst) was presented. If a monkey released the lever within 750 ms of offset of the respond stimulus, this was classified as a "correct rejection" and the monkey received a water reward (*top*). If he did not release the lever or released it after 750 ms (as depicted), this was a "false alarm" (*bottom*). The schematics of the different stimuli are cartoons and are not meant to represent the actual voltage-time waveforms of the tone-in-noise, noise-only, and respond stimuli.

Neural Recording Methodology

At the beginning of each experimental session, a tungsten electrode (1 MΩ at 1 kHz; FHC) or a multicontact linear-array electrode (U-Probe; Plexon; 16 electrode contacts) was lowered through a recording chamber and into the brain using a skull-mounted microdrive (model MO-97; Narishige). OpenEx (TDT), LabView (National Instruments), and MATLAB (The MathWorks) software synchronized behavioral control with stimulus production and data collection. Neural signals were sampled at 24 kHz, amplified (RA16PA and RZ2; TDT), and stored for online and offline analyses. Online spike sorting was conducted using OpenSorter (TDT).

Recording Strategy

Once a recording site was identified, we calculated the site's best frequency from the passive-listening paradigm. The frequency of the target stimulus was then set to the best frequency of the recording site; if we isolated multiple single neurons, we used the average best frequency across all of these neurons. The monkeys participated in randomly interleaved target-in-noise and noise-only trials. To accurately assess the monkeys' bias (response criterion), we presented approximately the same number of target-in-noise trials and noise-only trials. During target-in-noise trials, we randomly varied TNR on a trial-by-trial basis.

Behavioral Analyses

A psychometric function quantified the monkey's performance during the target-in-noise task. The independent variable of this function was TNR, and the dependent variable was the probability (P) that the monkeys released the lever following offset of the target-in-noise stimulus (i.e., hit rate). We fit the psychometric data to the integral of the Weibull function (Quick 1974): $P = \gamma + (1 - \gamma - \lambda) \cdot \{1 - \exp[-(\mathrm{TNR}/\alpha)^{\beta}]\}$. α (threshold, the TNR corresponding to $P = 0.75$ when $\gamma = 0.5$ and $\lambda = 0$), β (which governed the shape of the function), γ (the false alarm rate), and λ (the lapse rate, which is the fraction of misses for high-TNR stimuli and accounts for lapses of attention and other nonperceptual errors) were free parameters that were fit with a maximum-likelihood procedure.

Neural Analyses

We limited our neural analyses to the spiking activity elicited by the target-in-noise and noise-only stimuli and did not analyze neural responses that were elicited by the respond stimulus. Neural signals were re-sorted offline into single units using Offline Sorter (Plexon). Data are reported as firing rate (i.e., number of spikes per second) and were aligned relative to the onset of the target-in-noise stimulus or the noise-only stimulus. The "stimulus" period was the 750-ms period that began with onset of either *1*) the target-in-noise stimulus or *2*) the noise-only stimulus.

Definition of stimulus-responsive neurons. A neuron was considered "stimulus responsive" if its firing rate was modulated significantly during the stimulus period (across all TNRs of target-in-noise hit trials and noise-only correct-rejection trials), relative to a 750-ms baseline period that preceded stimulus onset (Wilcoxon rank-sum test, H_0: no median difference in firing rate between the baseline and stimulus periods, $P < 0.05$). We further subdivided this set of stimulus-responsive neurons into those that were "excited" and those that were "suppressed." An excited A1 neuron had a higher firing rate during the stimulus period, relative to the baseline period (1-tailed Wilcoxon rank-sum test, H_0: no difference in median firing rate, $P < 0.025$). A suppressed A1 neuron had a lower firing rate during the stimulus period, relative to the baseline period (1-tailed Wilcoxon rank-sum test, H_0: no difference in median firing rate, $P < 0.025$).

Neurometric function to test for TNR sensitivity. A neurometric analysis quantified the probability that an ideal observer could use firing rate alone to correctly detect the target stimulus as a function of TNR. The advantage of this analysis is that it allows for a direct comparison between neural sensitivity and behavioral (psychometric) sensitivity. The neurometric function relates the probability that an

ideal observer could use only a neuron's firing rate to correctly detect the target stimulus as a function of TNR. We only used correct trials (hits and correct rejections) to ensure that changes in neural activity reflected changes in TNR and were not conflated with changes in activity reflective of choice.

The neurometric curve is computed by first finding the firing rate value (i.e., a decision boundary) that best classified firing rates from target-in-noise trials (across all TNRs) into "signal" trials and firing rates from noise-then-response trials into "noise" trials. This boundary minimized the number of times that *1*) a firing-rate value from a noise-only trial could be misclassified as signal and *2*) a firing-rate value from a target-in-noise trial could be misclassified as noise. Next, on a trial-by-trial basis and as a function of TNR, we used this boundary to calculate the fraction of target-in-noise trials that were classified correctly as signal. That is, a firing rate value from a target-in-noise trial was classified as signal if it fell on the correct side of the boundary. Typically, for excited neurons, this would mean that its firing rate was greater than the boundary value. This boundary was fixed and was not recalculated for different TNRs. Finally, this function (i.e., the fraction of target-in-noise trials that were correctly classified as signal as a function of TNR) was fit to a logistic equation analogous to that described in *Behavioral Analyses*. We conducted this curve fitting using a variety of different fitting rules and start-stop criteria to test the degree to which different fits affected our findings. We found that, on average, our curve fits were robust to differences in the fitting quality in specific neurons.

Neurometric curves were calculated from time-binned spike rate data (bin duration: 50 ms, advanced in 50-ms increments, relative to onset of the target-in-noise stimulus). From the logistic fit, we calculated "neurometric sensitivity." Neurometric sensitivity is a measure of sensitivity to TNR, which depends on β (see logistic equation in *Behavioral Analyses*) and governs the steepness of the neurometric curve (steeper slopes reflected higher sensitivity). Neurometric sensitivity was defined as the slope of the function determined from the 25% and 75% detection choice points (Klein 2001; Tsunada et al. 2016).

Neural sensitivity to signal and noise. We used a receiver operating characteristic (ROC) analysis to calculate the degree to which an ideal observer could differentiate between firing rates elicited on signal trials from those on noise trials. The rationale for this analysis was that it more closely approximated the monkeys' task goals of distinguishing between signal trials (i.e., target-in-noise trials, independent of TNR) and noise trials (i.e., noise-only trials) and not detecting differences in TNR level like was indexed by the aforementioned neurometric analysis. The area under the ROC curve is the probability that an ideal observer could discriminate between the distribution of firing rates elicited on signal trials and those on noise trials.

In this analysis, firing rates were calculated, on a neuron-by-neuron basis, across the entire 750-ms stimulus period, and we used only data from correct trials (target-in-noise hit trials and noise-only correct-rejection trials). A bootstrap randomization procedure, which shuffled the relationship between firing rate and trial type (signal and noise) tested whether each neuron's ROC value was significantly different from chance (2-tailed permutation test, H_0: ROC value = 0.5, $P < 0.05$). We also tested whether the fraction of neurons with significant ROC values was reliable (binomial test, H_0: fraction of significant neurons equal to that expected by chance, $P < 0.05$).

Neural sensitivity to behavioral choice (choice probability). Choice probability quantifies the ability of an ROC-based ideal observer to determine a listener's choice based only on the firing rate of a single neuron, given responses separated by choice for nominally identical stimulus conditions (Britten et al. 1996; Gu et al. 2007; Purushothaman and Bradley 2005; Russ et al. 2008b; Tsunada et al. 2011, 2016). We computed choice probability from data generated in response to noise-only trials. Specifically, we tested the difference between the firing rate distributions generated on correct-rejection trials (i.e., the monkey did not report the presence of a target) and on false-alarm trials (i.e., the monkey reported the presence of a target). On a neuron-by-neuron basis, we analyzed choice probability in two different ways: *1*) as a function of time, using time-binned (bin duration: 100 ms, advanced in 50-ms increments) firing rate data, and *2*) across the entire 750-ms stimulus period. For this latter analysis, a bootstrap randomization procedure, which shuffled the relationship between firing rate and trial outcome (correct rejections and false alarms), tested whether each neuron's choice-probability value was significantly different from chance (2-tailed permutation test, H_0: choice probability = 0.5, $P < 0.05$). We also tested whether the fraction of neurons with significant choice-probability values was reliable (binomial test, H_0: fraction of significant neurons equal to that expected by chance, $P < 0.05$).

Population analyses: linear classifiers. Next, in two different analyses, we used a linear classifier to test whether the spiking activity of populations of A1 neurons contained more robust representations of the task parameters than the average (median) spiking activity of single A1 neurons. *1*) In the first analysis, we developed a linear classifier that quantified the degree to which the firing rates of A1 neural populations discriminated between signal (i.e., the firing rates on target-in-noise hit trials, independent of TNR) and noise (i.e., the firing rates on noise-only correct-rejection trials). We conducted this analysis because the monkeys' task goal was to report the presence of the signal and ignore noise but not to discriminate between different TNRs. In this analysis, we only used hit and correct-rejection trials to ensure that the results of the classifier were not conflated with choice effects. *2*) In the second linear classifier, we quantified how well the firing rates of populations of A1 neurons differentiated between the firing rates elicited on trials in which the monkeys made different behavioral choices, for the same nominal stimulus. Specifically, we compared population-level firing rate activity generated on correct-rejection trials with those from false-alarm trials.

Several methodological issues are worth noting. First, because different numbers of trials might have occurred for different trial or stimulus conditions, we subsampled our data to ensure that that we had the same number of trials for each condition (Blagus and Lusa 2010). Second, to control for potential bias due to neuron-by-neuron differences in firing rate, we *z*-scored each neuron's firing rate, which was calculated from the entire 750-ms stimulus period. Third, neuronal data were analyzed independent of recording session and monkey. As a consequence of this random selection, we minimized the contribution of correlation structure on the population read out, a practice consistent with several previous studies (Pagan et al. 2013; Rust and DiCarlo 2010, 2012). Finally, similarly to previous studies (Downer et al. 2017; Jazayeri and Movshon 2006; Miller and Recanzone 2009; Yang and Lisberger 2009), we set the frequency of the target stimulus at each neuron's best frequency. As a consequence, our population of A1 neurons was recorded using different stimuli. In other words, our analysis focused on population-level contributions of neurons that were tuned for the frequency of the target stimulus and minimized contributions of neurons with tuning curves that "flank" that frequency of the target stimulus. These latter two points are discussed further in DISCUSSION.

For each classification analysis (Carruthers et al. 2015; Pagan et al. 2013; Rust and DiCarlo 2010, 2012), we constructed an *N*-dimensional population response vector that constituted the firing rates of a population of *N* neurons to *R* repetitions of *S* stimulus conditions (e.g., signal and noise). Each classification analysis underwent a 10-fold cross-validation procedure to avoid overfitting. This procedure divided the neural data into 10 groups: in an iterative fashion, 1 group was a test set, and the remaining 9 formed a training set. To test how well each neural population could discriminate between the different trial or stimulus conditions, we implemented a linear read-out procedure in which we fit the training set to a linear hyperplane that separated the population response vectors corresponding to two different conditions (i.e., signal and noise or correct rejection and false alarms). Using this hyperplane, we calculated the fraction of times

that the test data was classified correctly and report average performance over 500 different instantiations of a classifier, which was constructed from N randomly selected neurons.

All classifiers were constructed using a support vector machine procedure that was implemented in the MATLAB programming environment using the LIBSVM library (Chang and Lin 2011) with a linear kernel, the C-SVC algorithm, and cost set to 1, which is the algorithm's default value.

RESULTS

Behavioral Performance

Monkeys S ($n = 48$ sessions) and *A* ($n = 11$ sessions) reliably reported the presence of a target stimulus (i.e., a tone burst) that was presented simultaneously in a noisy background of comodulated broadband noise (Fig. 2), with performance that depended systematically on TNR (Fig. 3). When the target stimulus was less than the sound level of the noise (i.e., TNR −5 dB, Fig. 3*A*), the monkey rarely reported the target. However, as the TNR increased, the fraction of times that the monkeys correctly reported the presence of the target increased (Fig. 3*A*). The monkey's false alarm rate was 8%.

Figure 3*B* replots the monkeys' performance as a function of d'. d' is a nonparametric measure of the monkeys' sensitivity in detecting the target stimulus (Green and Swets 1966). At the lowest TNR, the monkeys' average d' value was essentially zero, meaning that they could not discriminate between the target-in-noise stimulus and the noise stimulus. As TNR increased, their d' value increased, indicating their increased sensitivity to TNR.

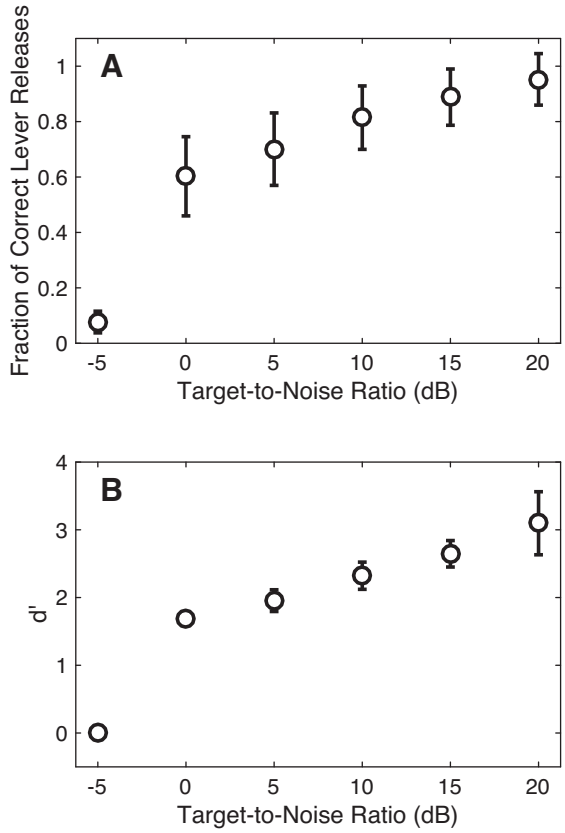

Fig. 3. Psychophysical performance. Behavioral data are plotted as the fraction of trials in which the monkey released the lever as a function of TNR during target-in-noise trials (i.e., hit rate; *A*) and as a function of d' (*B*). d' was calculated from the hit rate and from the proportion of false-alarm trials during the noise-only trials. Error bars are SD calculated using behavioral data from all of the recording sessions reported in this study.

Recording Site Localization

During these behavioral sessions, we isolated 116 single units from A1 in *monkey S* and 90 single units from A1 in *monkey A*. Because the data from *monkey A* were collected mostly with a multicontact electrode array, we could record from a comparable number of neurons with fewer recording sessions than in *monkey S*. The subsequent neurophysiological analyses were conducted only on stimulus-responsive neurons. Of the 206 single units, we classified 146 as stimulus responsive. We further subdivided these stimulus-responsive neurons into 120 excited neurons; an excited neuron had a higher firing rate during the stimulus period than during the baseline period (1-tailed Wilcoxon rank-sum test, H_0: no median difference in firing rate, $P < 0.025$). We also identified 26 suppressed neurons, which had higher firing rates during the baseline period than during the stimulus period (1-tailed Wilcoxon rank-sum test, H_0: no median difference in firing rate, $P < 0.025$).

We found that the frequency tuning of our population of A1 neurons ranged between 0.535 and 8.0 kHz (median: 1.32 kHz, interquartile range: 1.1–2.3 kHz). The median Q value (an index of tuning sharpness; best frequency divided by bandwidth, 10 dB above the lowest sound level that elicited a reliable response) was 3.5 (interquartile range: 2.3–4.6). Using spiking data across all TNRs and from all target-in-noise hit trials, we found that the median latency (i.e., the first of 2 or more consecutive time bins that were >2 SD above a 750-ms baseline period) was 29 ms. Median latency decreased to 20 ms when it was calculated only from the TNR value that elicited the maximum firing rate. This collection of neurophysiological response properties and our MRI-guided identification of A1's stereotactic location are consistent with those seen in earlier studies of A1 (Camalier et al. 2012; Fu et al. 2004; Kajikawa et al. 2005; Kikuchi et al. 2010; Massoudi et al. 2015; O'Connell et al. 2014; Recanzone et al. 1993, 1999, 2000; Werner-Reiss and Groh 2008) and verified our targeted recording site.

A1 Activity During the Target-in-Noise Task

The firing rates of A1 neurons were modulated by the stimuli of the target-in-noise task. For example, the spiking activity of the example A1 neurons in Fig. 4, *A* and *C*, had close to monotonic relationships between firing rate and TNR. For these neurons, the firing rate was lowest during presentation of the noise-only stimulus (gray curve; correct-rejection trials only) and then increased smoothly as we increased the TNR of the target-in-noise stimulus (colored curves; hit trials only). On the other hand, some neurons only seemed to code the presence of an auditory stimulus in the environment. For these neurons, all of the target-in-noise stimuli as well as the noise-only stimulus elicited nominally the same firing rate. One neuron with this response profile is shown in Fig. 5*A*. This neuron responded robustly and equally well to both the noise-only stimulus (gray data; correct rejections) and the target-in-noise stimuli (colored data; hits only). Other A1 neurons had firing

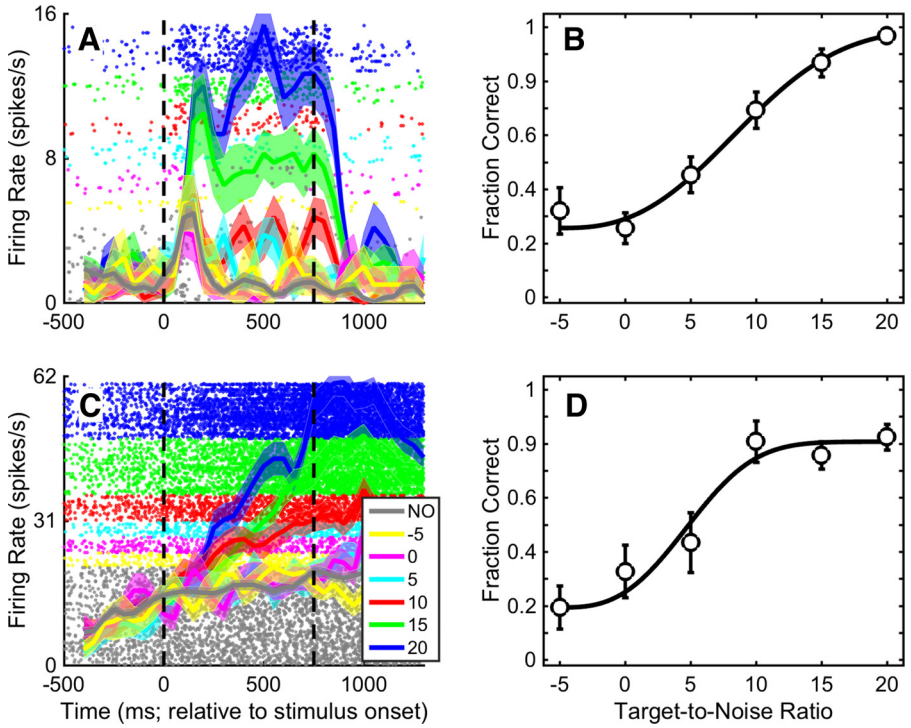

Fig. 4. Example A1 neurons whose firing rate was increased with TNR. *S*hown are data for 2 different A1 neurons whose firing rate was modulated relatively smoothly by TNR. *A* and *C*: raster plot and peristimulus time histogram for each neuron. Dots indicate the time of occurrence of action potentials relative to stimulus onset (*time 0*). Solid thick lines indicate the mean instantaneous firing rate (shading indicates ±SE) in 100-ms bins that advance by 50 ms. Colors correspond to different values of TNR from target-in-noise hit trials; gray indicates noise-only (NO) correct-rejection trials. Vertical dashed lines indicate stimulus onset and offset, respectively. *B* and *D*: neurometric curve for each corresponding neuron. Each curve plots the fraction of trials in which an ideal observer could use the neuron's firing rate to correctly detect the target stimulus as a function of TNR. The curves were obtained from firing rate data averaged over the 750-ms stimulus period. Error bars indicate SD. The solid black line is the maximum-likelihood fit of the neurometric data to the integral of the Weibull function (Quick 1974).

rates that were suppressed by onset of the auditory stimuli. One example neuron is shown in Fig. 5*C*.

Population peristimulus time histograms showed qualitatively similar trends as these example units. For excited neurons (Fig. 6*A*), on average, the noise-only stimulus elicited the smallest response. The average A1 firing rate was higher in response to the target-in-noise stimuli than to the noise-only stimulus and increased as the TNR of the target-in-noise stimulus increased. Furthermore, and consistent with the example suppressed neuron (see Fig. 5*C*), average A1 activity for suppressed neurons was not systematically modulated by the noise-only and the target-in-noise stimuli (Fig. 6*B*).

Neurometric Function to Test for TNR Sensitivity

In our first analysis, we calculated each neuron's neurometric function, which describes the probability that an ideal observer could use a neuron's spiking activity to detect the target stimulus. More specifically, this analysis quantified how well this ideal observer could use firing rate to differentiate

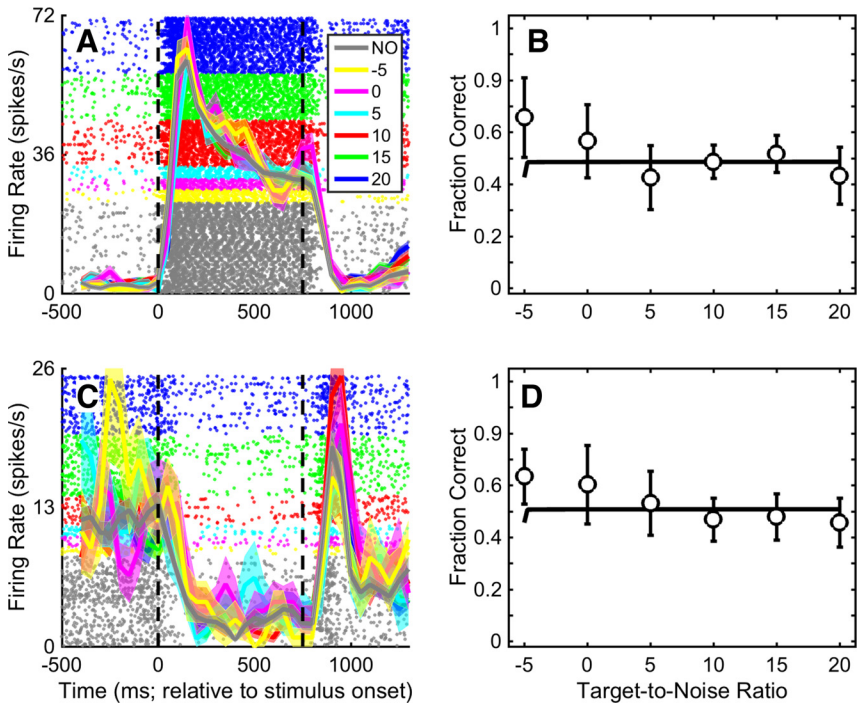

Fig. 5. Examples of an A1 neuron whose firing rate was not modulated by TNR and one whose firing rate was suppressed by TNR. Raster plots and peristimulus time histograms represent an A1 neuron whose firing rate was not differentially modulated by the different values of TNR of the target-in-noise stimulus and by the noise-only stimulus (*A*) and one whose firing rate was suppressed by TNR (*C*). Data in *B* and *D* show each neuron's corresponding neurometric function. The data are formatted in the same manner as Fig. 4.

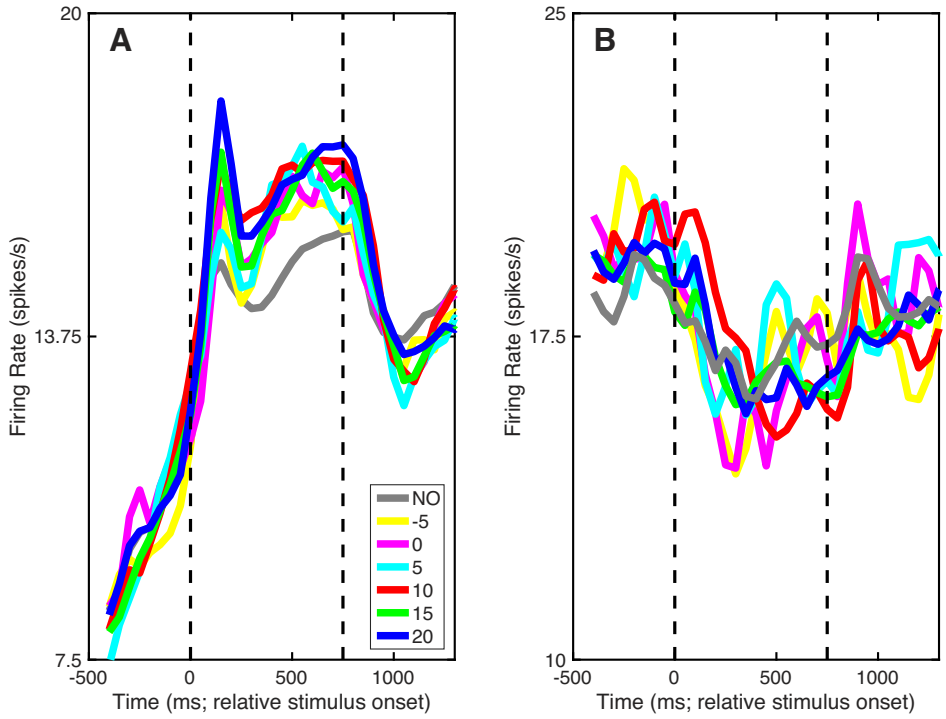

Fig. 6. Population activity. *A* and *B*: population peristimulus time histograms relative to stimulus onset. Solid lines indicate mean firing rate. Colors correspond to different values of TNR from target-in-noise hit trials; gray indicates noise-only (NO) correct-rejection trials. Vertical dashed lines indicate stimulus onset and offset, respectively. Data in *A* are from "excited" A1 stimulus-responsive neurons (i.e., those whose firing rate increased with stimulus onset). Data in *B* are from "suppressed" A1 stimulus-responsive neurons (i.e., those whose firing rate decreased with stimulus onset).

between target-in-noise trials and noise-only trials as a function of TNR; see MATERIALS AND METHODS for more details.

To put this neurometric analysis into context, consider our example neurons in Figs. 4 and 5. In Fig. 4, *A* and *C*, both neurons responded relatively weakly to the noise-only stimulus but responded with higher firing rates as we increased the TNR in the target-in-noise stimulus. Consequently, for their respective neurometric functions, we found that the fraction of times that an ideal observer could correctly detect the target stimulus increased with TNR and reached near perfect detectability at the highest TNR (+20 dB; Fig. 4, *B* and *D*).

In contrast, the response profile of the neuron in Fig. 5*A* is quite different. This neuron's firing rate was modulated strongly by the auditory stimuli but had nominally the same firing rate for all of the target-in-noise stimuli as well as for the noise-only stimulus. Because the neuron's firing was invariant to the different stimulus conditions, its neurometric curve (Fig. 5*B*) was essentially a flat line at ~0.5. In other words, the fraction of times that an ideal observer could use this neuron's spiking activity to detect the target stimulus was at chance level. Similarly, our example suppressed neuron (Fig. 5*C*) had a flat neurometric function (Fig. 5*D*), indicating, once again, that an ideal observer could not reliably use this neuron's firing rate to detect the target stimulus.

To quantify each neuron's sensitivity to TNR, we calculated the slope of each neuron's neurometric function: steeper slopes indicate more sensitivity to TNR than do shallower slopes. The slope of the function was determined from the 25% and 75% detection choice points (Δfraction correct/ΔTNR). Neurometric sensitivity was calculated as a function of time by using 50-ms bins of spiking data that advanced in 50-ms increments. We also examined neurometric sensitivity over the entire 750-ms stimulus period.

Scatter plots showing distributions of slope values as a function of time (relative to stimulus onset) are shown in Fig. 7*A*. Consistent with our observation that many A1 neurons were not substantially modulated by TNR (Fig. 6), many of these slopes were close to zero. However, we found that the median of each of these distributions was significantly greater than zero (Wilcoxon rank-sum test, H_0: median slope value = 0, $P < 0.05$). Although some of the individual distributions differed from one another (Kruskal-Wallis test, H_0: median slope difference equals = 0, $P < 0.05$), we could not identify a consistent pattern.

An important benefit of calculating the neurometric slope is that we can compare this value with an analogous value derived from the psychometric function. This comparison provides insight into the degree to which A1 activity correlates with the monkeys' behavior. Neurometric slopes [median for the entire stimulus period: 0.036 (Δfraction correct/ΔTNR); interquartile range: 0.02–0.05] were shallower (Wilcoxon signed-rank test, H_0: median slope value = 0, $P < 0.05$) than the corresponding psychometric slopes [median: 0.067 (Δfraction correct/ΔTNR); interquartile range: 0.05–0.07].

ROC Analysis to Test for Sensitivity to Signal and Noise

All of the above-described analyses quantified the degree to which neural activity encoded the different values of TNR. However, the monkeys' task was not to explicitly report these values or to discriminate between different TNR values. Thus, although it is informative to look at TNR sensitivity, a better measure may be to quantify the sensitivity of A1 activity to the monkeys' actual task goal: that is, detect signal (i.e., all target-in-noise trials), independent of TNR value, and ignore noise (i.e., noise-only trials). To test neural sensitivity to this signal vs. noise discrimination, we conducted an ROC analysis, which quantified how well an ideal observer could discriminate between A1 spiking activity elicited on signal and noise trials.

The result of this ROC analysis is shown in Fig. 7*B*. The median value of this distribution was 0.51 (range: 0.23–1,

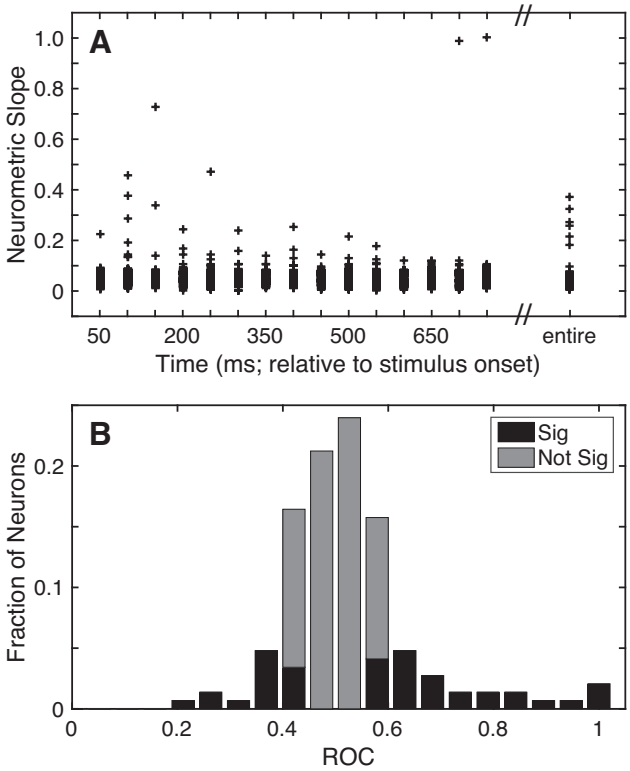

Fig. 7. Selectivity of A1 responses. *A*: neurometric sensitivity to TNR. Sensitivity was defined as the slope (Δfraction correct/ΔTNR) of each neuron's neurometric function from the 25% and 75% detection choice points. Neurometric sensitivity is shown as a scatter plot as a function of time (relative to stimulus onset) using 50-ms bins of data that advanced in 50-ms increments, as well as the entire 750-ms stimulus period (*far right*). *B*: discriminability between "signal" and "noise". The discriminability between the firing rates elicited on signal and noise trials was calculated with an ROC ideal-observer analysis on a neuron-by-neuron basis. Bar graph shows the distribution of ROC values. Black bars indicate those neurons with significant (Sig) ROC values (2-tailed permutation test, H_0: ROC value = 0.5, $P < 0.05$). Gray bars indicate those that did not have significant (Not Sig) ROC values (2-tailed permutation test, H_0: ROC value = 0.5, $P > 0.05$).

interquartile range: 0.45–0.57), a value that was not different from chance (Wilcoxon rank-sum test, H_0: median ROC value = 0.5, $P > 0.05$). That is, an ideal observer, in general, could not use the firing rate of A1 neurons to discriminate between the firing rates elicited on signal and noise trials. Yet, we found that certain A1 neurons (44/146; 30%) had ROC values that differed from chance (2-tailed permutation test, H_0: ROC value = 0.5, $P < 0.05$), a percentage that was higher than expected by chance (binomial test, H_0: fraction of significant neurons equal to that expected by chance: 7.3%, $P < 0.05$).

Choice Probability

To test the relationship between A1 activity and the monkeys' decisions, we computed the choice probability of individual neurons (Fig. 8). Choice probability quantifies the ability of an ROC-based ideal observer to use the spiking activity of A1 neurons to discriminate between the monkeys' choices for the same nominal stimulus. On a neuron-by-neuron basis and as a function of time (100-ms bins that advanced over time in 50-ms increments), we found that the median choice-probability value did not differ from chance (Wilcoxon rank-sum, H_0: median choice-probability value = 0.5, $P > 0.05$; Fig. 8*A*).

We also tested, on a neuron-by-neuron basis, choice probability using the entire 750-ms stimulus period (Fig. 8*B*). Because the median value of this choice-probability distribution (0.51; interquartile range: 0.47–0.54) did not differ from chance (Wilcoxon rank-sum test, H_0: median choice-probability value = 0.5, $P > 0.05$), it indicates that we could not identify any systematic effect of choice on the spiking activity of individual A1 neurons. However, a population of A1 neurons (14/146; 9.5%) had choice-probability values that differed from chance (2-tailed permutation test, H_0: choice-probability value = 0.5, $P < 0.05$), a fraction that was higher than expected by chance (binomial test, H_0: percentage of significant neurons equal to that expected by chance: 7.3%, $P < 0.05$).

In an additional analysis, we correlated, on a neuron-by-neuron basis, choice probability and neurometric sensitivity (i.e., neurometric slope, calculated over the entire 750-ms stimulus period). We could not identify a relationship between these two values (Fig. 8*C*; Spearman correlation coefficient = −0.042, $P > 0.05$). Similarly, an analysis between the

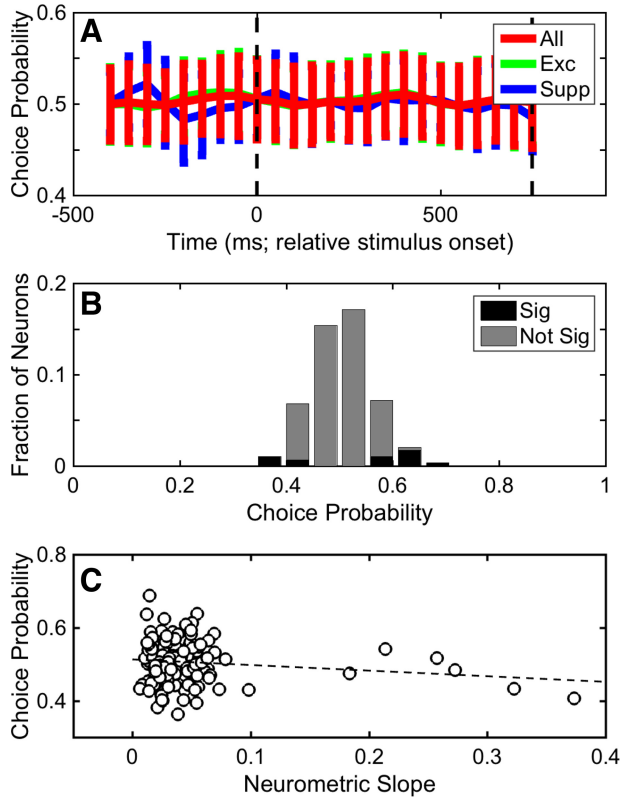

Fig. 8. Distribution of choice probability. Distribution of choice probabilities was calculated as a function of time (*A*) and over the entire 750-ms stimulus period (*B*). *A*: data were calculated using firing rates that were binned into 100-ms bins that advance in 50-ms increments. Each data point is the mean choice-probability value, and error bars indicate SD. Choice probability was calculated independently using the entire set of A1 stimulus-responsive neurons (red), the subpopulation of excited stimulus-responsive neurons (green), and the subpopulation of suppressed stimulus-responsive neurons (blue). *B*: black bars indicate the fraction with significant (Sig) choice-probability values (2-tailed permutation test, H_0: choice probability = 0.5, $P < 0.05$). Gray bars indicate the fraction that did not have significant (Not Sig) choice-probability values (2-tailed permutation test, H_0: choice probability = 0.5, $P > 0.05$). *C*: neurometric slope (Δfraction correct/ΔTNR) is correlated with choice-probability value on a neuron-by-neuron basis. Dashed line shows the correlation line between these two values; this correlation was not significant (Spearman $r = -0.042$; $P > 0.05$). The slope values were generated from data collected over the entire 750-ms stimulus period; see Fig. 7.

ROC values (Fig. 7*B*) and behavioral d' (Fig. 3*B*) failed to identify a relationship. These findings suggest that, in general, even the most sensitive A1 neurons did not have task-driven activity that was related to the monkeys' choices (Britten et al. 1996; Celebrini and Newsome 1994; Gu et al. 2007; Law and Gold 2008; Tsunada et al. 2016).

Population Decoding of A1 Activity

Single-neuron analyses can provide important insights but may not necessarily predict the contribution of an A1 neural population, as a whole, to auditory behavior (Ince et al. 2013; Mesgarani et al. 2008; Miller and Recanzone 2009). To test how population-level A1 spiking activity encoded variables related to our target-in-noise task, we constructed cross-validated linear classifiers (support vector machines) (Pagan et al. 2013; Rust and DiCarlo 2010, 2012) and tested whether we could use a linear-decision boundary to separate A1 population activity elicited by *1*) signal and noise or *2*) different behavioral reports. The results of these classifier analyses are shown in Fig. 9.

In our first analysis, we constructed a linear classifier and tested how well A1 population activity differentially encoded signal (i.e., target-in-noise trials, across all TNRs) and noise (noise-only trials). We chose to do this analysis because the monkeys' task goal was to report the presence of the signal and ignore noise but not to discriminate between different TNRs. The results of this classifier are shown in Fig. 9*A*. The firing rates of individual A1 neurons discriminated between signal and noise trials with an accuracy of ~0.6; this value is somewhat comparable to the 0.51 median value that we found in our single-neuron ROC analysis; see Fig. 7*B*). However, as the size of the A1 population increased, the performance of the classifier improved and approached near-perfect classification with 100 neurons. The subpopulation of excited A1 neurons tracked with the entire A1 population. However, the subpopulation of suppressed A1 neurons did not vary much from chance performance.

Next, we constructed a second classifier and tested whether this classifier could discriminate between A1 population spiking activity elicited by different behavioral reports for nominally identical stimuli. We used neural activity elicited by the noise-only stimulus of the noise-only task and tested whether a classifier could discriminate between correct-rejection and false-alarm trials. The results of this classifier are shown in Fig. 9*B*. Comparable to our single-neuron choice-probability findings (Fig. 8), the average decoding capacity of the classifier for single neurons was at chance level (i.e., 0.5). As the size of the A1 neural population increased, the decoding capacity increased and was able to discriminate between correct rejections and false alarms with a maximum accuracy of ~0.75. This decoding capacity was mainly attributable to the excited subpopulation of A1 neurons; the decoding capacity of the suppressed A1 neurons hovered at ~0.5.

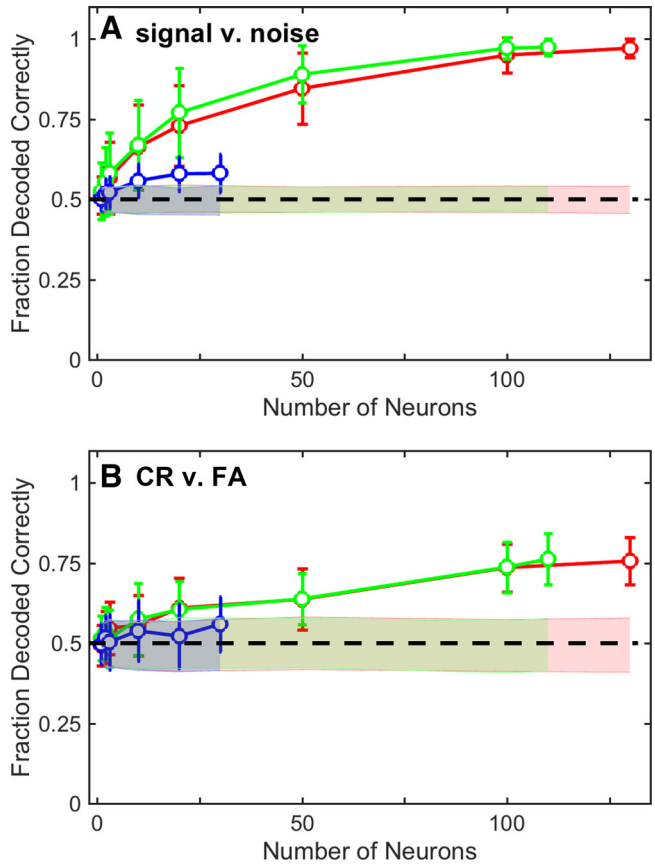

Fig. 9. Population analysis of A1. A decoding analysis (linear classifier) quantified how well increasingly larger populations of A1 neurons encoded "signal" (i.e., the distribution of firing rates generated during target-in-noise hit trials across all TNRs) vs. "noise" (i.e., the distribution of firing rates generated during noise-only correct-rejection trials) (*A*) and choice [correct rejections (CR) vs. false alarms (FA); *B*]. Independent decoding analyses were conducted using the entire set of A1 stimulus-responsive neurons (red), the subpopulation of excited neurons (green), and the subpopulation of suppressed neurons (blue). Circles indicate the mean performance of each classifier (i.e., the fraction of times that the classifier correctly classified the test data); error bars indicate SD. Shaded regions indicate the mean (±95% confidence interval) classifier performance expected by chance (bootstrap randomization procedure). Dashed lines in *A* and *B* indicate chance performance.

DISCUSSION

We combined, for the first time in a nonhuman-primate model, behavior and neural recordings to identify a potential contribution of A1 spiking activity to a listener's ability to detect a target sound from a noisy background. This study tested the contribution of A1 to a listener's detection of a target stimulus whose onset and offset co-occur with a noisy background (see Fig. 2). An open empirical question is the degree to which the current findings are limited to this type of task or whether they generalize to other types of tasks, such as the detection of a target from an ongoing noisy background.

We found that as TNR increased, the probability that the monkeys reported the target increased (Fig. 3). Our monkeys' performance was comparable to that reported in similar nonhuman primate studies (Bohlen et al. 2014; Dylla et al. 2013). Any behavioral differences between the current and the previous monkey studies most likely relate to differences in how the monkeys were trained and differences in task design (e.g., reward structure, proportion of noise trials, etc.). For example, one potentially important difference between the current and previous studies is that we kept the TNR values constant and did not vary these values based on changes in the monkeys' psychometric threshold. Furthermore, because we did not systematically vary the properties of the noise-only stimulus (e.g., the phase onset of the amplitude modulation), we could not deduce the strategy that the monkeys used to solve our task.

However, a recent study indicated that monkeys detect a target in a noisy background by listening in the "dips" of the comodulated noise (i.e., the time points when the amplitude of the noise was minimized) (Bohlen et al. 2014).

Three points are worth discussing with respect to our patterns of spiking activity. First, one interesting phenomenon, which was apparent in individual single neurons (e.g., Fig. 4*C*) and in population spiking activity of the excited neurons (Fig. 6), was that spiking activity appeared to ramp up during the baseline period (i.e., the time before stimulus onset). We eliminated several trivial explanations for this ramping. For example, this activity was not due to acausal filtering. That is, it was not due to a large smoothing kernel that averaged pre- and peristimulus responses together. Similarly, it is not due to poor spike sorting: after an independent resorting of the spiking data, we still found this ramping. It may very well be that because our prestimulus period had a fixed duration, the monkeys might have been able to "time" the onset of the stimulus. We speculate that this increase in prestimulus activity reflects the monkeys' anticipation of stimulus onset, a possibility that is consistent with increasing evidence that A1 activity can correlate with behavioral and task demands (Bizley et al. 2013; Brosch et al. 2005; 2011; Fritz et al. 2003; Jaramillo and Zador 2011; Johnson et al. 2012; King and Nelken 2009; Lakatos et al. 2013, 2016; Lee and Middlebrooks 2011; Niwa et al. 2012a, 2012b; Otazu et al. 2009; Recanzone and Sutter 2008; Selezneva et al. 2006; Vaadia et al. 1982; Werner-Reiss et al. 2003). Second, like previous studies that identified beautifully synchronized (time-locked) responses to amplitude-modulated noise (Lu et al. 2001; Lu and Wang 2000; Niwa et al. 2012a, 2012b, 2013), we also found synchronized activity (median vector strength = 0.16; interquartile range: 0.09–0.23; TNR = 20 dB; (Goldberg and Brown 1969). This degree of synchronization appears somewhat less than that seen in these previous studies. One possible explanation for this discrepancy is that because our monkeys were trained on only one amplitude-modulation depth (100% sinusoidally amplitude modulated noise), there might have been stimulus-responsive plasticity that minimized the occurrence of this synchronization. Third, like several other central auditory system studies (Bar-Yosef and Nelken 2007; Delgutte and Kiang 1984; Giraud et al. 1997; May et al. 1998; Mesgarani et al. 2014; Narayan et al. 2007; Schneider and Woolley 2013; Scott and McGettigan 2013; Shetake et al. 2011; Wong et al. 2008), the spiking activity of A1 neurons was modulated modestly and to differing degrees by TNR (Figs. 4, 5, and 7*A*), suggestive of non-monotonic sound-level tuning (Sadagopan and Wang 2008). However, it is inconsistent with that seen from anesthetized subjects in which most neurons had monotonic sound-level tuning (Phillips and Hall 1986).

How did A1 activity relate to behavior? The slopes of our neurometric curves were, on average, relatively shallow. Moreover, they were shallower than the corresponding psychophysical sensitivity. This difference in slope indicates that single A1 neurons could not, on average, account for the monkeys' behavior. This finding is consistent with our ROC analysis (Fig. 7*B*) in which we found that the firing rate of the median A1 neuron did not differentiate between signal and noise trials. Similarly, the monkeys' choices did not modulate the firing rate of the median A1 neuron (Fig. 8). Together, these three analyses suggest that the average (median) spiking activity of single neurons in A1 may not be sufficient to explain the monkeys' behavior in our target-in-noise task.

However, population-level analyses revealed that relatively small groups of neurons more closely matched the monkeys' performance (Fig. 9). For example, with populations of ~20 neurons, the fraction of signal and noise trials that were decoded correctly was ~0.75 (Fig. 9*A*). This value closely mirrored the monkeys' overall performance: on average, the monkeys were able to successfully report the target (signal) on ~0.68 of trials (across all TNRs; Fig. 3). With larger neuronal populations, classifier performance continued to improve and actually exceeded the monkeys' performance. Populations of ~100 A1 neurons also reflected the monkeys' choices (Fig. 9*B*).

One potential interpretation of this finding is that individual A1 neurons were weakly sensitive to different task-related parameters, but as a population, A1 neurons robustly represented the parameter space of our target-in-noise task appropriately. In other words, if spiking activity in all A1 neurons identically represented the parameters of our target-in-noise task, then the population-level analyses would be identical to the single-neuron analyses. However, because population-level activity more closely mirrors behavioral activity, it suggests that the spiking activity of different A1 neurons represents the appropriate parameter space sufficiently enough to explain the monkeys' behavior during our task.

This notion that populations of neurons have a more robust representation of task-related information than single neurons is consistent with several previous studies (Averbeck et al. 2006; DiCarlo et al. 2012; Downer et al. 2015; Engineer et al. 2008; Graf et al. 2011; Ince et al. 2013; Kohn et al. 2016; Pachitariu et al. 2015; Pouget et al. 2000; Safaai et al. 2013). For example, seminal studies by Middlebrooks and colleagues (Middlebrooks et al. 1994, 1998; Stecker and Middlebrooks 2003; Xu et al. 1998) and more recent work by Miller and Recanzone (2009) have identified population codes in the auditory cortex that can subserve sound-localization behavior. In those studies, average single-unit activity from auditory cortex neurons was relatively broadly tuned for the location of a sound source. Because the spatial sensitivity of these individual neurons was much broader than a listener's behavioral sensitivity, it was unclear how individual neurons could serve as a basis for spatial perception. However, the sensitivity of this population-level activity was comparable to the listener's behavioral sensitivity and could potentially subserve behavior. Similarly, population codes have been shown to be important in the encoding of vocalizations and speech sounds (Chang et al. 2010; Engineer et al. 2008; Fishman et al. 2016; Ince et al. 2013; Mizrahi et al. 2014; Pasley et al. 2012; Russ et al. 2008a; Schneider and Woolley 2013). We add to this literature by identifying a population-level contribution of primate A1 spiking activity to a nonspatial perceptual decision.

Nonetheless, any interpretation of our population analysis needs to be couched by several important caveats. First, in the construction of our classifiers, we included all of our neurons and treated them equivalently. It is not clear, though, whether the brain reads out all neurons equivalently. Indeed, it may very well be that downstream neurons only read out the most informative neurons (Ince et al. 2013; Law and Gold 2008), for example, those neurons whose firing rate was modulated to the greatest extent (and/or most reliably) by different values of

TNR or only those neurons whose tuning properties matched the frequency of the target stimulus (Downer et al. 2017; Jazayeri and Movshon 2006; Miller and Recanzone 2009; Yang and Lisberger 2009). Second, the degree to which access to larger populations of A1 neurons affects decoding cannot be readily determined without knowing the exact process by which A1 activity is read out. Third, whereas our decoder used a linear algorithm (DiCarlo et al. 2012), it may very well be that actual neurons use nonlinear decoding. Fourth, we did not include timing information in our classifier and focused on firing rates only. Incorporating this spike-timing information might have increased the accuracy of their performance (Middlebrooks et al. 1994, 1998; Stecker and Middlebrooks 2003; Xu et al. 1998). Finally, as is common in nonhuman-primate auditory studies (but see Atencio and Schreiner 2008, 2010; Fishman and Steinschneider 2012; Lakatos et al. 2008, 2013; Schroeder and Lakatos 2009; Schroeder et al. 2010; Tsunada et al. 2012), we do not know whether we recorded from the same cortical layer or from different cortical layers, and we cannot conclusively determine whether we recorded from different neuronal classes. It is possible that if we had been able to identify the layer and/or neuronal class, a subset of our recordings (e.g., those in a certain layer) might have had response properties that more directly related to the detection process required in our task.

In addition to the caveats noted above, is not clear why classifier performance with larger neuronal populations was better than the monkeys' behavioral performance. However, one likely possibility is the effect of interneuronal correlations on population activity. Correlated activity can substantially affect neural sensitivity and the read out of population activity (Cohen and Kohn 2011; Cohen and Newsome 2009; Downer et al. 2015; Graf et al. 2011; Gu et al. 2011; Kohn et al. 2016; Liu et al. 2013; Zohary et al. 1994). Because we ignored the correlation structure (see MATERIALS AND METHODS), like other prominent studies (DiCarlo and Cox 2007; DiCarlo et al. 2012; Miller and Recanzone 2009; Pagan et al. 2013; Rust and DiCarlo 2012), we may have inflated the read-out capacity of our neural population. Nonetheless, because we simultaneously measured auditory behavior and neural activity, unlike previous studies that did not simultaneously collect these measures (Ince et al. 2013; Mizrahi et al. 2014; Narayan et al. 2007; Russ et al. 2008a; Schneider and Woolley 2013; Shetake et al. 2011), we were able to describe, for the first time, the degree to which population-level A1 activity might support auditory perception.

Finally, our population analyses only indicate that information is available in A1 population activity. It is a substantially different question to ask whether downstream neurons can read out this information and create representations at the level of the single neuron that can match behavior or whether this information remains encoded at the population level. To address this question, we need more studies that systematically investigate how populations of neurons in different cortical regions of the ventral auditory pathway encode and represent perceptually relevant features of our auditory world (DiCarlo and Cox 2007; DiCarlo et al. 2012; Miller and Recanzone 2009; Rust and DiCarlo 2012).

How do our single-neuron and population-level findings fit into the broader A1 literature? Even though A1 is classically considered to be a general processor of auditory information, there is increasingly more evidence suggesting that perceptual and task-related information is found in the spiking activity of A1 neurons (Bizley et al. 2013; Brosch et al. 2005; 2011; Fritz et al. 2003; Jaramillo and Zador 2011; Johnson et al. 2012; King and Nelken 2009; Lakatos et al. 2013, 2016; Lee and Middlebrooks 2011; Niwa et al. 2012a, 2012b; Otazu et al. 2009; Recanzone and Sutter 2008; Selezneva et al. 2006; Vaadia et al. 1982; Werner-Reiss et al. 2003). In contrast, the current findings and previous work from our group and others suggest that the monkeys' auditory decisions (choices) do not reliably modulate neural activity in the auditory cortex (Binder et al. 2004; Chang et al. 2010; Gutschalk et al. 2008; Lemus et al. 2009; Tsunada et al. 2011, 2016). However, it is conceivable that in those studies, as we showed in the current study (Fig. 9), choice-related signals may have been present in population-level activity.

Nonetheless, at present, we cannot fully reconcile these different sets of findings. However, one possibility may relate to the specific nature of the auditory decision. For those studies that demonstrated significant choice-related spiking activity in A1 (Bizley et al. 2011; Niwa et al. 2012b; 2013), it may be that A1 contributes directly to the decision process because the relevant stimulus attributes were represented robustly in the firing rates of individual A1 neurons or in earlier levels of auditory processing (Pressnitzer et al. 2008; Yao et al. 2015). In contrast, in the current study and in other studies that did not identify choice-related spiking activity in the auditory cortex (Lemus et al. 2009; Tsunada et al. 2011, 2016), later regions of the ventral auditory pathway encode choice because single A1 neurons do not robustly represent the relevant stimulus features. Indeed, single-neuron and functional imaging studies have demonstrated that areas beyond auditory cortex can be modulated by choice during certain tasks, including those that require listening in noisy backgrounds (Binder et al. 2004; Russ et al. 2008b; Salvi et al. 2002). Thus the functional contribution of each brain region of the ventral pathway to auditory perception may be modulated by the specific nature and demands of the decision (Bizley and Cohen 2013; Bizley et al. 2011; Niwa et al. 2013).

An important caveat to this discussion is that the presence of A1 choice-related spiking activity in our studies or in previous (monkey and ferret) studies (Bizley et al. 2011; Niwa et al. 2012a, 2012b, 2013) does not necessarily imply that it arises in A1, nor is it part of a feedforward process in which this choice-related activity contributes causally to the eventual auditory decision (Nienborg and Cumming 2009; Niwa et al. 2013; Tsunada et al. 2016). Similar neural signatures might also arise from regions of the ventral auditory pathway that represent the auditory decision but provide feedback connections back to A1 (Nienborg and Cumming 2009). Future work should focus on using auditory response-time tasks (Stüttgen et al. 2011; Tsunada et al. 2016) to identify the temporal window of an auditory decision to differentiate between these feedforward vs. feedback alternatives (Cohen and Newsome 2009; Nienborg and Cumming 2009).

ACKNOWLEDGMENTS

We thank Joshua Gold, Nicole Rust, Maria Geffen, Marino Pagan, and Heather Hersh for suggestions on the preparation of this manuscript and Harry Shirley for outstanding veterinary support.

GRANTS

This research was supported by National Institute of Deafness and Other Communications Disorders Grants 5R03DC012431, 5R01DC013961, and 5R01DC009224 (Y. E. Cohen, S. Bennur) and the Boucai Hearing Restoration Fund (Y. E. Cohen).

DISCLOSURES

No conflicts of interest, financial or otherwise, are declared by the authors.

AUTHOR CONTRIBUTIONS

K.L.C.-L., S.B., and Y.E.C. conceived and designed research; K.L.C.-L., S.B., and Y.E.C. analyzed data; K.L.C.-L., S.B., and Y.E.C. interpreted results of experiments; K.L.C.-L., S.B., and Y.E.C. prepared figures; K.L.C.-L., S.B., and Y.E.C. drafted manuscript; K.L.C.-L., S.B., and Y.E.C. edited and revised manuscript; K.L.C.-L., S.B., and Y.E.C. approved final version of manuscript; S.B. performed experiments.

REFERENCES

Atencio CA, Schreiner CE. Spectrotemporal processing differences between auditory cortical fast-spiking and regular-spiking neurons. *J Neurosci* 28: 3897–3910, 2008. doi:10.1523/JNEUROSCI.5366-07.2008.

Atencio CA, Schreiner CE. Columnar connectivity and laminar processing in cat primary auditory cortex. *PLoS One* 5: e9521, 2010. doi:10.1371/journal.pone.0009521.

Averbeck BB, Latham PE, Pouget A. Neural correlations, population coding and computation. *Nat Rev Neurosci* 7: 358–366, 2006. doi:10.1038/nrn1888.

Bar-Yosef O, Nelken I. The effects of background noise on the neural responses to natural sounds in cat primary auditory cortex. *Front Comput Neurosci* 1: 3, 2007. doi:10.3389/neuro.10.003.2007.

Binder JR, Liebenthal E, Possing ET, Medler DA, Ward BD. Neural correlates of sensory and decision processes in auditory object identification. *Nat Neurosci* 7: 295–301, 2004. doi:10.1038/nn1198.

Bizley JK, Cohen YE. The what, where and how of auditory-object perception. *Nat Rev Neurosci* 14: 693–707, 2013. doi:10.1038/nrn3565.

Bizley JK, Walker DK, Nodal FR, King AJ, Schnupp J. Neural correlates of pitch discrimination during passive and active listening. Program No. 173.04. *2011 Neuroscience Meeting Planner*. Washington, DC: Society for Neuroscience, 2011.

Bizley JK, Walker KM, Nodal FR, King AJ, Schnupp JW. Auditory cortex represents both pitch judgments and the corresponding acoustic cues. *Curr Biol* 23: 620–625, 2013. doi:10.1016/j.cub.2013.03.003.

Blagus R, Lusa L. Class prediction for high-dimensional class-imbalanced data. *BMC Bioinformatics* 11: 523, 2010. doi:10.1186/1471-2105-11-523.

Bohlen P, Dylla M, Timms C, Ramachandran R. Detection of modulated tones in modulated noise by non-human primates. *J Assoc Res Otolaryngol* 15: 801–821, 2014. doi:10.1007/s10162-014-0467-7.

Britten KH, Newsome WT, Shadlen MN, Celebrini S, Movshon JA. A relationship between behavioral choice and the visual responses of neurons in macaque MT. *Vis Neurosci* 13: 87–100, 1996. doi:10.1017/S095252380000715X.

Bronkhorst AW. The cocktail party phenomenon: a review of research on speech intelligibility in multiple-talker conditions. *Acustica* 86: 117–128, 2000.

Bronkhorst AW, Plomp R. Effect of multiple speechlike maskers on binaural speech recognition in normal and impaired hearing. *J Acoust Soc Am* 92: 3132–3139, 1992. doi:10.1121/1.404209.

Brosch M, Selezneva E, Scheich H. Nonauditory events of a behavioral procedure activate auditory cortex of highly trained monkeys. *J Neurosci* 25: 6797–6806, 2005. doi:10.1523/JNEUROSCI.1571-05.2005.

Brosch M, Selezneva E, Scheich H. representation of reward feedback in primate auditory cortex. *Front Syst Neurosci* 5: 5, 2011. doi:10.3389/fnsys.2011.00005.

Camalier CR, D'Angelo WR, Sterbing-D'Angelo SJ, de la Mothe LA, Hackett TA. Neural latencies across auditory cortex of macaque support a dorsal stream supramodal timing advantage in primates. *Proc Natl Acad Sci USA* 109: 18168–18173, 2012. doi:10.1073/pnas.1206387109.

Carruthers IM, Laplagne DA, Jaegle A, Briguglio JJ, Mwilambwe-Tshilobo L, Natan RG, Geffen MN. Emergence of invariant representation of vocalizations in the auditory cortex. *J Neurophysiol* 114: 2726–2740, 2015. doi:10.1152/jn.00095.2015.

Celebrini S, Newsome WT. Neuronal and psychophysical sensitivity to motion signals in extrastriate area MST of the macaque monkey. *J Neurosci* 14: 4109–4124, 1994.

Chang CC, Lin CJ. LIBSVM: a library for support vector machine. *ACM Trans Intell Syst Technol* 2: 27, 2011. doi:10.1145/1961189.1961199.

Chang EF, Rieger JW, Johnson K, Berger MS, Barbaro NM, Knight RT. Categorical speech representation in human superior temporal gyrus. *Nat Neurosci* 13: 1428–1432, 2010. doi:10.1038/nn.2641.

Cohen MR, Kohn A. Measuring and interpreting neuronal correlations. *Nat Neurosci* 14: 811–819, 2011. doi:10.1038/nn.2842.

Cohen MR, Newsome WT. Estimates of the contribution of single neurons to perception depend on timescale and noise correlation. *J Neurosci* 29: 6635–6648, 2009. doi:10.1523/JNEUROSCI.5179-08.2009.

Delgutte B, Kiang NY. Speech coding in the auditory nerve: V. Vowels in background noise. *J Acoust Soc Am* 75: 908–918, 1984. doi:10.1121/1.390537.

DiCarlo JJ, Cox DD. Untangling invariant object recognition. *Trends Cogn Sci* 11: 333–341, 2007. doi:10.1016/j.tics.2007.06.010.

DiCarlo JJ, Zoccolan D, Rust NC. How does the brain solve visual object recognition? *Neuron* 73: 415–434, 2012. doi:10.1016/j.neuron.2012.01.010.

Downer JD, Niwa M, Sutter ML. Task engagement selectively modulates neural correlations in primary auditory cortex. *J Neurosci* 35: 7565–7574, 2015. doi:10.1523/JNEUROSCI.4094-14.2015.

Downer JD, Niwa M, Sutter ML. Hierarchical differences in population coding within auditory cortex. *J Neurophysiol* 118: 717–731, 2017. doi:10.1152/jn.00899.2016.

Dylla M, Hrnicek A, Rice C, Ramachandran R. Detection of tones and their modification by noise in nonhuman primates. *J Assoc Res Otolaryngol* 14: 547–560, 2013. doi:10.1007/s10162-013-0384-1.

Engineer CT, Perez CA, Chen YH, Carraway RS, Reed AC, Shetake JA, Jakkamsetti V, Chang KQ, Kilgard MP. Cortical activity patterns predict speech discrimination ability. *Nat Neurosci* 11: 603–608, 2008. doi:10.1038/nn.2109.

Fishman YI, Micheyl C, Steinschneider M. Neural representation of concurrent vowels in macaque primary auditory cortex. *eNeuro* 3: 3, 2016. doi:10.1523/ENEURO.0071-16.2016.

Fishman YI, Steinschneider M. Searching for the mismatch negativity in primary auditory cortex of the awake monkey: deviance detection or stimulus specific adaptation? *J Neurosci* 32: 15747–15758, 2012. doi:10.1523/JNEUROSCI.2835-12.2012.

Fritz J, Shamma S, Elhilali M, Klein D. Rapid task-related plasticity of spectrotemporal receptive fields in primary auditory cortex. *Nat Neurosci* 6: 1216–1223, 2003. doi:10.1038/nn1141.

Fu KM, Shah AS, O'Connell MN, McGinnis T, Eckholdt H, Lakatos P, Smiley J, Schroeder CE. Timing and laminar profile of eye-position effects on auditory responses in primate auditory cortex. *J Neurophysiol* 92: 3522–3531, 2004. doi:10.1152/jn.01228.2003.

Giraud AL, Garnier S, Micheyl C, Lina G, Chays A, Chéry-Croze S. Auditory efferents involved in speech-in-noise intelligibility. *Neuroreport* 8: 1779–1783, 1997.

Goldberg JM, Brown PB. Response of binaural neurons of dog superior olivary complex to dichotic tonal stimuli: some physiological mechanisms of sound localization. *J Neurophysiol* 32: 613–636, 1969.

Graf AB, Kohn A, Jazayeri M, Movshon JA. Decoding the activity of neuronal populations in macaque primary visual cortex. *Nat Neurosci* 14: 239–245, 2011. doi:10.1038/nn.2733.

Green DM, Swets JA. *Signal Detection Theory and Psychophysics*. New York: John Wiley and Sons, 1966.

Gu Y, DeAngelis GC, Angelaki DE. A functional link between area MSTd and heading perception based on vestibular signals. *Nat Neurosci* 10: 1038–1047, 2007. doi:10.1038/nn1935.

Gu Y, Liu S, Fetsch CR, Yang Y, Fok S, Sunkara A, DeAngelis GC, Angelaki DE. Perceptual learning reduces interneuronal correlations in macaque visual cortex. *Neuron* 71: 750–761, 2011. doi:10.1016/j.neuron.2011.06.015.

Gutschalk A, Micheyl C, Oxenham AJ. Neural correlates of auditory perceptual awareness under informational masking. *PLoS Biol* 6: e138, 2008. doi:10.1371/journal.pbio.0060138.

Ince RA, Panzeri S, Kayser C. Neural codes formed by small and temporally precise populations in auditory cortex. *J Neurosci* 33: 18277–18287, 2013. doi:10.1523/JNEUROSCI.2631-13.2013.

Jaramillo S, Zador AM. The auditory cortex mediates the perceptual effects of acoustic temporal expectation. *Nat Neurosci* 14: 246–251, 2011. doi:10.1038/nn.2688.

Jazayeri M, Movshon JA. Optimal representation of sensory information by neural populations. *Nat Neurosci* 9: 690–696, 2006. doi:10.1038/nn1691.

Johnson JS, Yin P, O'Connor KN, Sutter ML. The ability of primary auditory cortical neurons to detect amplitude modulation with rate and temporal codes: neurometric analysis. *J Neurophysiol* 107: 3325–3341, 2012. doi:10.1152/jn.00812.2011.

Kajikawa Y, de La Mothe L, Blumell S, Hackett TA. A comparison of neuron response properties in areas A1 and CM of the marmoset monkey auditory cortex: tones and broadband noise. *J Neurophysiol* 93: 22–34, 2005. doi:10.1152/jn.00248.2004.

Kikuchi Y, Horwitz B, Mishkin M. Hierarchical auditory processing directed rostrally along the monkey's supratemporal plane. *J Neurosci* 30: 13021–13030, 2010. doi:10.1523/JNEUROSCI.2267-10.2010.

King AJ, Nelken I. Unraveling the principles of auditory cortical processing: can we learn from the visual system? *Nat Neurosci* 12: 698–701, 2009. doi:10.1038/nn.2308.

Klein SA. Measuring, estimating, and understanding the psychometric function: a commentary. *Percept Psychophys* 63: 1421–1455, 2001. doi:10.3758/BF03194552.

Kohn A, Coen-Cagli R, Kanitscheider I, Pouget A. Correlations and neuronal population information. *Annu Rev Neurosci* 39: 237–256, 2016. doi:10.1146/annurev-neuro-070815-013851.

Lakatos P, Barczak A, Neymotin SA, McGinnis T, Ross D, Javitt DC, O'Connell MN. Global dynamics of selective attention and its lapses in primary auditory cortex. *Nat Neurosci* 19: 1707–1717, 2016. doi:10.1038/nn.4386.

Lakatos P, Karmos G, Mehta AD, Ulbert I, Schroeder CE. Entrainment of neuronal oscillations as a mechanism of attentional selection. *Science* 320: 110–113, 2008. doi:10.1126/science.1154735.

Lakatos P, Musacchia G, O'Connel MN, Falchier AY, Javitt DC, Schroeder CE. The spectrotemporal filter mechanism of auditory selective attention. *Neuron* 77: 750–761, 2013. doi:10.1016/j.neuron.2012.11.034.

Las L, Stern EA, Nelken I. Representation of tone in fluctuating maskers in the ascending auditory system. *J Neurosci* 25: 1503–1513, 2005. doi:10.1523/JNEUROSCI.4007-04.2005.

Law CT, Gold JI. Neural correlates of perceptual learning in a sensory-motor, but not a sensory, cortical area. *Nat Neurosci* 11: 505–513, 2008. doi:10.1038/nn2070.

Lee CC, Middlebrooks JC. Auditory cortex spatial sensitivity sharpens during task performance. *Nat Neurosci* 14: 108–114, 2011. doi:10.1038/nn.2713.

Lee JH, Russ BE, Orr LE, Cohen YE. Prefrontal activity predicts monkeys' decisions during an auditory category task. *Front Integr Neurosci* 3: 16, 2009. doi:10.3389/neuro.07.016.2009.

Lemus L, Hernández A, Romo R. Neural codes for perceptual discrimination of acoustic flutter in the primate auditory cortex. *Proc Natl Acad Sci USA* 106: 9471–9476, 2009. doi:10.1073/pnas.0904066106.

Liu S, Gu Y, DeAngelis GC, Angelaki DE. Choice-related activity and correlated noise in subcortical vestibular neurons. *Nat Neurosci* 16: 89–97, 2013. doi:10.1038/nn.3267.

Lu T, Liang L, Wang X. Neural representations of temporally asymmetric stimuli in the auditory cortex of awake primates. *J Neurophysiol* 85: 2364–2380, 2001.

Lu T, Wang X. Temporal discharge patterns evoked by rapid sequences of wide- and narrowband clicks in the primary auditory cortex of cat. *J Neurophysiol* 84: 236–246, 2000.

Massoudi R, Van Wanrooij MM, Versnel H, Van Opstal AJ. Spectrotemporal response properties of core auditory cortex neurons in awake monkey. *PLoS One* 10: e0116118, 2015. doi:10.1371/journal.pone.0116118.

May BJ, Prell GS, Sachs MB. Vowel representations in the ventral cochlear nucleus of the cat: effects of level, background noise, and behavioral state. *J Neurophysiol* 79: 1755–1767, 1998.

Mesgarani N, David SV, Fritz JB, Shamma SA. Phoneme representation and classification in primary auditory cortex. *J Acoust Soc Am* 123: 899–909, 2008. doi:10.1121/1.2816572.

Mesgarani N, David SV, Fritz JB, Shamma SA. Mechanisms of noise robust representation of speech in primary auditory cortex. *Proc Natl Acad Sci USA* 111: 6792–6797, 2014. doi:10.1073/pnas.1318017111.

Middlebrooks JC, Clock AE, Xu L, Green DM. A panoramic code for sound location by cortical neurons. *Science* 264: 842–844, 1994. doi:10.1126/science.8171339.

Middlebrooks JC, Xu L, Eddins AC, Green DM. Codes for sound-source location in nontonotopic auditory cortex. *J Neurophysiol* 80: 863–881, 1998.

Miller LM, Recanzone GH. Populations of auditory cortical neurons can accurately encode acoustic space across stimulus intensity. *Proc Natl Acad Sci USA* 106: 5931–5935, 2009. doi:10.1073/pnas.0901023106.

Mizrahi A, Shalev A, Nelken I. Single neuron and population coding of natural sounds in auditory cortex. *Curr Opin Neurobiol* 24: 103–110, 2014. doi:10.1016/j.conb.2013.09.007.

Moore DR, Edmondson-Jones M, Dawes P, Fortnum H, McCormack A, Pierzycki RH, Munro KJ. Relation between speech-in-noise threshold, hearing loss and cognition from 40-69 years of age. *PLoS One* 9: e107720, 2014. doi:10.1371/journal.pone.0107720.

Narayan R, Best V, Ozmeral E, McClaine E, Dent M, Shinn-Cunningham B, Sen K. Cortical interference effects in the cocktail party problem. *Nat Neurosci* 10: 1601–1607, 2007. doi:10.1038/nn2009.

Nelken I, Rotman Y, Bar Yosef O. Responses of auditory-cortex neurons to structural features of natural sounds. *Nature* 397: 154–157, 1999. doi:10.1038/16456.

Nienborg H, Cumming BG. Decision-related activity in sensory neurons reflects more than a neuron's causal effect. *Nature* 459: 89–92, 2009. doi:10.1038/nature07821.

Niwa M, Johnson JS, O'Connor KN, Sutter ML. Active engagement improves primary auditory cortical neurons' ability to discriminate temporal modulation. *J Neurosci* 32: 9323–9334, 2012a. doi:10.1523/JNEUROSCI.5832-11.2012.

Niwa M, Johnson JS, O'Connor KN, Sutter ML. Activity related to perceptual judgment and action in primary auditory cortex. *J Neurosci* 32: 3193–3210, 2012b. doi:10.1523/JNEUROSCI.0767-11.2012.

Niwa M, Johnson JS, O'Connor KN, Sutter ML. Differences between primary auditory cortex and auditory belt related to encoding and choice for AM sounds. *J Neurosci* 33: 8378–8395, 2013. doi:10.1523/JNEUROSCI.2672-12.2013.

O'Connell MN, Barczak A, Schroeder CE, Lakatos P. Layer specific sharpening of frequency tuning by selective attention in primary auditory cortex. *J Neurosci* 34: 16496–16508, 2014. doi:10.1523/JNEUROSCI.2055-14.2014.

Otazu GH, Tai LH, Yang Y, Zador AM. Engaging in an auditory task suppresses responses in auditory cortex. *Nat Neurosci* 12: 646–654, 2009. doi:10.1038/nn.2306.

Pachitariu M, Lyamzin DR, Sahani M, Lesica NA. State-dependent population coding in primary auditory cortex. *J Neurosci* 35: 2058–2073, 2015. doi:10.1523/JNEUROSCI.3318-14.2015.

Pagan M, Urban LS, Wohl MP, Rust NC. Signals in inferotemporal and perirhinal cortex suggest an untangling of visual target information. *Nat Neurosci* 16: 1132–1139, 2013. doi:10.1038/nn.3433.

Pasley BN, David SV, Mesgarani N, Flinker A, Shamma SA, Crone NE, Knight RT, Chang EF. Reconstructing speech from human auditory cortex. *PLoS Biol* 10: e1001251, 2012. doi:10.1371/journal.pbio.1001251.

Pfingst BE, Hienz R, Miller J. Reaction-time procedure for measurement of hearing. II. Threshold functions. *J Acoust Soc Am* 57: 431–436, 1975. doi:10.1121/1.380466.

Phillips DP, Hall SE. Spike-rate intensity functions of cat cortical neurons studied with combined tone-noise stimuli. *J Acoust Soc Am* 80: 177–187, 1986. doi:10.1121/1.394178.

Pomeranz J, Kubovy M. Theoretical approaches to perceptual organization. In: *Handbook of Perception and Human Performance*, edited by Boff KR, Kauffman L, and Thomas JP. New York: Wiley, 1986, vol. 2, p. 1–46.

Pouget A, Dayan P, Zemel R. Information processing with population codes. *Nat Rev Neurosci* 1: 125–132, 2000. doi:10.1038/35039062.

Pressnitzer D, Sayles M, Micheyl C, Winter IM. Perceptual organization of sound begins in the auditory periphery. *Curr Biol* 18: 1124–1128, 2008. doi:10.1016/j.cub.2008.06.053.

Purushothaman G, Bradley DC. Neural population code for fine perceptual decisions in area MT. *Nat Neurosci* 8: 99–106, 2005. doi:10.1038/nn1373.

Quick RF Jr. A vector-magnitude model of contrast detection. *Kybernetik* 16: 65–67, 1974. doi:10.1007/BF00271628.

Rauschecker JP, Scott SK. Maps and streams in the auditory cortex: nonhuman primates illuminate human speech processing. *Nat Neurosci* 12: 718–724, 2009. doi:10.1038/nn.2331.

Recanzone GH, Guard DC, Phan ML. Frequency and intensity response properties of single neurons in the auditory cortex of the behaving macaque monkey. *J Neurophysiol* 83: 2315–2331, 2000.

Recanzone GH, Schreiner CE, Merzenich MM. Plasticity in the frequency representation of primary auditory cortex following discrimination training in adult owl monkeys. *J Neurosci* 13: 87–103, 1993.

Recanzone GH, Schreiner CE, Sutter ML, Beitel RE, Merzenich MM. Functional organization of spectral receptive fields in the primary auditory cortex of the owl monkey. *J Comp Neurol* 415: 460–481, 1999. doi:10.1002/(SICI)1096-9861(19991227)415:4<460::AID-CNE4>3.0.CO;2-F.

Recanzone GH, Sutter ML. The biological basis of audition. *Annu Rev Psychol* 59: 119–142, 2008. doi:10.1146/annurev.psych.59.103006.093544.

Romanski LM. Representation and integration of auditory and visual stimuli in the primate ventral lateral prefrontal cortex. *Cereb Cortex* 17, *Suppl* 1: i61–i69, 2007. doi:10.1093/cercor/bhm099.

Russ BE, Ackelson AL, Baker AE, Cohen YE. Coding of auditory-stimulus identity in the auditory non-spatial processing stream. *J Neurophysiol* 99: 87–95, 2008a. doi:10.1152/jn.01069.2007.

Russ BE, Orr LE, Cohen YE. Prefrontal neurons predict choices during an auditory same-different task. *Curr Biol* 18: 1483–1488, 2008b. doi:10.1016/j.cub.2008.08.054.

Rust NC, Dicarlo JJ. Selectivity and tolerance ("invariance") both increase as visual information propagates from cortical area V4 to IT. *J Neurosci* 30: 12978–12995, 2010. doi:10.1523/JNEUROSCI.0179-10.2010.

Rust NC, DiCarlo JJ. Balanced increases in selectivity and tolerance produce constant sparseness along the ventral visual stream. *J Neurosci* 32: 10170–10182, 2012. doi:10.1523/JNEUROSCI.6125-11.2012.

Sadagopan S, Wang X. Level invariant representation of sounds by populations of neurons in primary auditory cortex. *J Neurosci* 28: 3415–3426, 2008. doi:10.1523/JNEUROSCI.2743-07.2008.

Safaai H, von Heimendahl M, Sorando JM, Diamond ME, Maravall M. Coordinated population activity underlying texture discrimination in rat barrel cortex. *J Neurosci* 33: 5843–5855, 2013. doi:10.1523/JNEUROSCI.3486-12.2013.

Salvi RJ, Lockwood AH, Frisina RD, Coad ML, Wack DS, Frisina DR. PET imaging of the normal human auditory system: responses to speech in quiet and in background noise. *Hear Res* 170: 96–106, 2002. doi:10.1016/S0378-5955(02)00386-6.

Schneider DM, Woolley SM. Sparse and background-invariant coding of vocalizations in auditory scenes. *Neuron* 79: 141–152, 2013. doi:10.1016/j.neuron.2013.04.038.

Schroeder CE, Lakatos P. The gamma oscillation: master or slave? *Brain Topogr* 22: 24–26, 2009. doi:10.1007/s10548-009-0080-y.

Schroeder CE, Wilson DA, Radman T, Scharfman H, Lakatos P. Dynamics of active sensing and perceptual selection. *Curr Opin Neurobiol* 20: 172–176, 2010. doi:10.1016/j.conb.2010.02.010.

Scott SK, McGettigan C. The neural processing of masked speech. *Hear Res* 303: 58–66, 2013. doi:10.1016/j.heares.2013.05.001.

Selezneva E, Scheich H, Brosch M. Dual time scales for categorical decision making in auditory cortex. *Curr Biol* 16: 2428–2433, 2006. doi:10.1016/j.cub.2006.10.027.

Shetake JA, Wolf JT, Cheung RJ, Engineer CT, Ram SK, Kilgard MP. Cortical activity patterns predict robust speech discrimination ability in noise. *Eur J Neurosci* 34: 1823–1838, 2011. doi:10.1111/j.1460-9568.2011.07887.x.

Stecker GC, Middlebrooks JC. Distributed coding of sound locations in the auditory cortex. *Biol Cybern* 89: 341–349, 2003. doi:10.1007/s00422-003-0439-1.

Stüttgen MC, Schwarz C, Jäkel F. Mapping spikes to sensations. *Front Neurosci* 5: 125, 2011. doi:10.3389/fnins.2011.00125.

Sutter ML, Shamma SA. The relationship of auditory cortical activity to perception and behavior. In: *The Auditory Cortex*, edited by Winer JA and Schreiner CE. New York: Springer, 2011, p. 617–641.

Tsunada J, Lee JH, Cohen YE. Representation of speech categories in the primate auditory cortex. *J Neurophysiol* 105: 2634–2646, 2011. doi:10.1152/jn.00037.2011.

Tsunada J, Lee JH, Cohen YE. Differential representation of auditory categories between cell classes in primate auditory cortex. *J Physiol* 590: 3129–3139, 2012. doi:10.1113/jphysiol.2012.232892.

Tsunada J, Liu AS, Gold JI, Cohen YE. Causal contribution of primate auditory cortex to auditory perceptual decision-making. *Nat Neurosci* 19: 135–142, 2016. doi:10.1038/nn.4195.

Vaadia E, Gottlieb Y, Abeles M. Single-unit activity related to sensorimotor association in auditory cortex of a monkey. *J Neurophysiol* 48: 1201–1213, 1982.

Werner-Reiss U, Groh JM. A rate code for sound azimuth in monkey auditory cortex: implications for human neuroimaging studies. *J Neurosci* 28: 3747–3758, 2008. doi:10.1523/JNEUROSCI.5044-07.2008.

Werner-Reiss U, Kelly KA, Trause AS, Underhill AM, Groh JM. Eye position affects activity in primary auditory cortex of primates. *Curr Biol* 13: 554–562, 2003. doi:10.1016/S0960-9822(03)00168-4.

Wong PC, Uppunda AK, Parrish TB, Dhar S. Cortical mechanisms of speech perception in noise. *J Speech Lang Hear Res* 51: 1026–1041, 2008. doi:10.1044/1092-4388(2008/075).

Xu L, Furukawa S, Middlebrooks JC. Sensitivity to sound-source elevation in nontonotopic auditory cortex. *J Neurophysiol* 80: 882–894, 1998.

Yang J, Lisberger SG. Relationship between adapted neural population responses in MT and motion adaptation in speed and direction of smooth-pursuit eye movements. *J Neurophysiol* 101: 2693–2707, 2009. doi:10.1152/jn.00061.2009.

Yao JD, Bremen P, Middlebrooks JC. Emergence of spatial stream segregation in the ascending auditory pathway. *J Neurosci* 35: 16199–16212, 2015. doi:10.1523/JNEUROSCI.3116-15.2015.

Zohary E, Shadlen MN, Newsome WT. Correlated neuronal discharge rate and its implications for psychophysical performance. *Nature* 370: 140–143, 1994. [Erratum. *Nature* 371: 358, 1994.] doi:10.1038/370140a0.